MANCHESTER
1824
The University of Manchester

The University of Manchester Research

# Photoluminescence efficiency of zincblende InGaN/GaN quantum wells

**DOI:**
10.1063/5.0046649

**Document Version**
Accepted author manuscript

Link to publication record in Manchester Research Explorer

**Citation for published version (APA):**
Church, S., Quinn, M., Cooley-Greene, K., Ding, B., Gundimeda, A., Kappers, M. J., Frentrup, M., Wallis, D., Binks, D., & Oliver, R. A. (2021). Photoluminescence efficiency of zincblende InGaN/GaN quantum wells. *Journal of Applied Physics*, *129*, Article 175702. https://doi.org/10.1063/5.0046649

**Published in:**
Journal of Applied Physics

**Citing this paper**
Please note that where the full-text provided on Manchester Research Explorer is the Author Accepted Manuscript or Proof version this may differ from the final Published version. If citing, it is advised that you check and use the publisher's definitive version.

**General rights**
Copyright and moral rights for the publications made accessible in the Research Explorer are retained by the authors and/or other copyright owners and it is a condition of accessing publications that users recognise and abide by the legal requirements associated with these rights.

**Takedown policy**
If you believe that this document breaches copyright please refer to the University of Manchester's Takedown Procedures [http://man.ac.uk/04Y6Bo] or contact uml.scholarlycommunications@manchester.ac.uk providing relevant details, so we can investigate your claim.

Download date:14. Oct. 2024

# Photoluminescence efficiency of zincblende InGaN/GaN quantum wells

S. A. Church,[1] M. Quinn,[1] K. Cooley-Greene,[1] B. Ding,[2] A. Gundimeda,[2] M. J. Kappers,[2] M. Frentrup,[2] D. J. Wallis,[2,3] R. A. Oliver,[2] and D. J. Binks[1,4]

[1)] *Department of Physics and Astronomy, Photon Science Institute, University of Manchester, Manchester M13 9PL, United Kingdom*

[2)] *Department of Materials Science and Metallurgy, University of Cambridge, 27 Charles Babbage Road, Cambridge CB3 0FS, United Kingdom*

[3)] *Centre for High Frequency Engineering, University of Cardiff, 5 The Parade, Newport Road, Cardiff, CF24 3AA, United Kingdom*

[4)] *Corresponding Author: david.binks@manchester.ac.uk*

Growing green and amber emitting InGaN/GaN quantum wells in the zincblende, rather than the wurtzite, crystal phase has the potential to improve efficiency. However, optimisation of the emission efficiency of these heterostructures is still required to compete with more conventional alternatives. Photoluminescence time decays were used to assess how the quantum well width and number of quantum wells affect the recombination rates, and temperature dependent photoluminescence was used to determine the factors affecting recombination efficiency. The radiative recombination lifetime was found to be approximately 600 ps and to increase weakly with well width, consistent with a change in the exciton binding energy. The relative efficiency at room temperature was found to increase by a factor of five when the number of wells was increased from one to five. Furthermore, the efficiency increased by factor 2.2 when the width was increased from 2.5 nm to 7.5 nm. These results indicate that thermionic emission is the most important process reducing efficiency at temperatures in excess of 100 K. Moreover, the weak dependence of the rate of radiative recombination on well width means that increasing well thickness is an effective way of suppressing thermionic emission and thereby increasing efficiency in zincblende InGaN/GaN quantum wells, in contrast to those grown in the wurtzite phase.

## I. INTRODUCTION

The active region of commercial white LEDs consists of a blue-emitting InGaN/GaN quantum well (QW) grown in the c-direction of the wurtzite (wz) crystal structure. The QWs can emit light with an internal quantum efficiency (IQE) of up to 90 %[1]. Some of this light is absorbed by a phosphor coating, which re-emits yellow light. At low drive currents, the device efficiency is limited by Stokes' losses from the phosphor[2]. This can be avoided by instead mixing the light from red, green and blue LEDs to produce white light where the efficiency is more closely related to the IQE of the active regions.

The emission wavelength of the InGaN/GaN QWs can be increased to the green and red by increasing the indium alloy fraction. However, in conventional wurtzite LEDs this leads to a reduction in the IQE[3]. This "green gap", is partially due to the strong electric fields which are present perpendicular to the QWs. These fields form due to the spontaneous and piezoelectric polarisation of the crystal structure, and results in a reduced electron-hole wavefunction overlap[4]. A higher indium content increases the strain in the QW and leads to stronger electric fields, and therefore reduced radiative recombination rates. Another important factor is the increase in the non-radiative recombination rate for higher indium content, which has been attributed to a greater density of point defects in the active region due to the low growth temperatures required to incorporate more indium[5].

Thus the efficiency of white LEDs could be improved by increasing the IQE of longer wavelength emitters by reducing either the required indium content or the electric field strength. Both of these can be achieved by growing the InGaN/GaN QWs in the zincblende (zb) instead of the wz phase. Firstly, the bandgap of zb-GaN is 200 meV smaller than that of wz-GaN[6], so longer wavelength emission can be achieved with a lower indium content[7]. Additionally, zb-GaN is free of polarisation fields in the [001] direction[8–10], which leads to faster radiative recombination rates due to excitonic recombination[8,11]. It may also be possible to use thicker zb-QWs to increase the emission wavelength[12], which is not feasible in polar-QWs due to the greater electron-hole separation produced as the QW thickness increases.

zb-GaN is typically grown heteroepitaxially on zb-structured substrates, such as GaAs[13] or 3C-SiC/Si (001)[14,15], the latter of which has the advantage of a reduced lattice mismatch with the GaN (3.4 %[16]). However, zb-GaN tends to have a high density of extended defects such as threading dislocations and stacking faults (SFs) [17–19] which may increase the non-radiative recombination rate.

To investigate the factors affecting the performance of zb-InGaN/GaN QWs, the photoluminescence (PL) from a series of zb-InGaN/GaN QWs with different QW widths and numbers of wells is investigated. The PL lifetimes and temperature dependence for these QWs are compared and used to assess the emission efficiency.

## II. EXPERIMENTAL METHODS

The samples studied in this paper, shown schematically in Figure 1, consist of five zb-InGaN/GaN QW

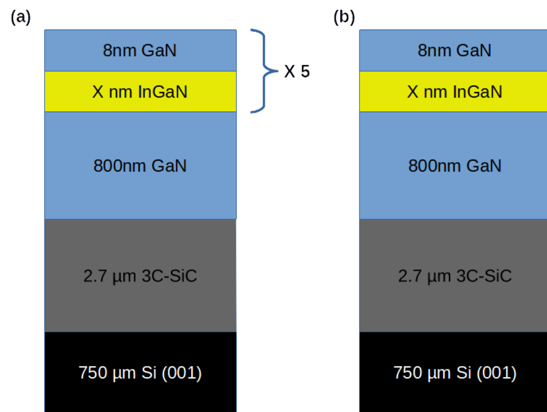


FIG. 1. A schematic diagram for five-QW samples studied in this paper, where X (2.5 nm, 5 nm, or 7.5 nm) is the QW thickness (a). A schematic for the single QW sample (b).

structures deposited on a 800 nm thick zb-GaN buffer layer. These heterostructures were grown in an Aixtron 1x6" MOVPE CCS reactor on 3C-SiC/Si (001) substrates as detailed in ref[20]. The InGaN/GaN MQW stack was grown under conditions typically used for (0001) MQW structures, as described in detail in ref[21]. The barrier width was nominally 8 nm and the QW-width was varied between samples, nominally 2.5 nm, 5.0 nm and 7.5 nm. A single QW was also grown with a QW-width of 2.5 nm under the same conditions. The structure of the single quantum well sample was examined by cross-sectional scanning transmission electron microscopy (STEM), using a FEI Tecnai Osiris microscope operated at 200 kV. High-angle annular dark-field (HAADF) STEM images were taken with the beam direction parallel to the [1-10] zone axis. The indium concentration was estimated from our luminescence studies rather than by x-ray diffraction, as explained below.

The optical properties of the QWs were investigated using temperature dependent PL spectroscopy. The samples were placed on the cold finger of a closed-cycle helium cryostat, capable of reducing the temperature to 10 K, and excited using a continuous wave He-Cd laser at a wavelength of 325 nm with an excitation power density of 10 W cm$^{-2}$. This photon energy is above the bandgap of GaN (3.3 eV[6]), and therefore photons are absorbed in both the GaN and the InGaN layers. The 1/e absorption length is approximately 80 nm[22,23], and so photons will be absorbed in the QWs, barriers and underlying GaN layers.

The luminescence was focused onto the slit of a spectrometer with a spectral resolution of 4.8 nm and detected using a GaAs photomultiplier tube. The spectral response of the system was measured using a calibrated black body and used to correct the spectra. A lock-in amplifier and optical chopper were used to extract and process the luminescence signal.

PL time decay measurements were performed with a 100 fs pulsed Ti:Sapphire laser, which was frequency tripled to a wavelength of 267 nm and produced a photogenerated carrier density of approximately $1 \times 10^{11}$ cm$^{-2}$pulse$^{-1}$. The luminescence was detected using a micro-channel plate with a 1/e time resolution of 80 ps, and time correlated single photon counting techniques were used to produce the PL transients.

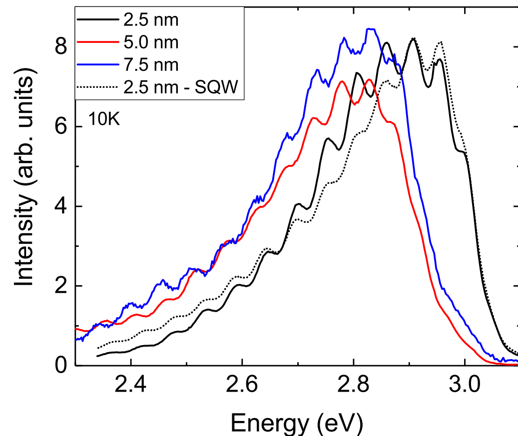


FIG. 2. Photoluminescence spectra of zb-InGaN/GaN QWs with different QW widths at a temperature of 10 K and an excitation power density of 10 W/cm$^2$. The oscillations of the intensity on these spectra are due to Fabry-Perot interference[24]. The peak intensity of the SQW sample has been normalised to that of the five QW samples.

## III. RESULTS

A (HAADF) STEM image of the SQW sample is given in the supplementary material (S.M.) as an example. It has been previously reported[25] that stacking faults (SFs) can cause significant buckling of zb-InGaN/GaN QWs and this is evident here as well. The non-planar geometry of the QWs produced by the buckling prevents a reliable analysis of composition by x-ray diffraction techniques. As discussed below, the indium content of the QWs and Qwires is instead estimated by comparing the peak emission energy to calculations of the recombination energy for different compositions.

PL spectra at a temperature of 10 K for the QW samples studied are shown in Fig. 2. The samples show emission in the visible spectrum originating from recombination in the InGaN/GaN QWs[11]. The peak recombination energy is between 2.8 eV and 2.9 eV. The FWHM of the spectra are 290 meV, 300 meV and 290 meV, and there is no trend observed with increasing QW width. The FWHM of the single QW sample spectrum is 280 meV, similar to the five-QWs, which suggests that inhomogeneity within each QW, rather than differences between the QWs in the stack, is the dominant source of variation.

Previous studies on zb-InGaN/GaN QWs have shown that the major source of inhomogeneity is the segregation of indium, which occurs in 2 nm wide regions in the QWs adjacent to SFs[25]. The local indium content in these regions can be enhanced by a factor of 2.3 and thus produce one-dimensional quantum wires (Qwires), with a size of 2nm in one direction and a size in an orthogonal direction that is limited by the QW width [25]. The impact of these Qwires has previously been observed in optical measurements: a second, lower energy, emission peak which is highly polarised at all temperatures[11]. There is only one emission peak in the spectra in this report, although polarisation-resolved PL spectra, shown in the S.M., show that the maximum degree of linear polarisation at 10 K is 69 %. This result is similar to the Qwire emission in previous samples[11] and suggests the emission described in this report is also predominantly due to recombination in these Qwire defects but, as indicated by a degree of linear polarisation at 10 K that is less than 100 %, with a contribution due to recombination in the QWs. Structural characterisation has shown that similar segregation is seen in zb-InGaN layers of different thicknesses[25]. It is therefore likely that the SF-related indium segregation is similar for all of the samples studied in this paper, consistent with their similar spectral width as seen in Fig. 2.

As the width of the QW is increased, the emission redshifts by 80 meV over the range studied. To both estimate the indium content and understand the origin of the redshift, the ground state electron-hole transition energies were calculated for the Qwires. The Qwires were treated as square potential wells that confine both electrons and holes in two dimensions. This potential well is 2 nm wide in one direction, corresponding to the width of the indium segregation region adjacent to an SF, and has a length equal to the QW thickness in an orthogonal direction. Note that the potential well could be treated as square since the zb-InGaN/GaN QWs in this study are free of the transverse electric fields that are present in wz-InGaN/GaN QWs[9]. Further details of these calculations are given in the S.M. and the results show that the transition energies are only weakly dependent on QW width for thicknesses greater than about 5 nm, in agreement with the very similar peak energies observed for the 5 nm and 7.5 nm QW samples, as shown in Fig 2. In contrast, the transition energies are more sensitive to the indium content, redshifting by about 30 meV for a 1 % change in indium content of the Qwire for a 5 nm wide well, for instance. These calculations also allow us to estimate the indium content in the Qwires as 20.0 % ± 0.5 % for the 5 nm and 7.5 nm samples, and 22.5 % ± 0.5 % for the 2.5 nm samples; these values correspond to indium contents of 9 % ± 5 % and 10 % ± 5 % in the rest of the QWs, respectively.

The PL time decays were measured at a temperature of 10 K and at intervals across each emission spectrum. The decays obtained at the PL peaks are shown as an inset in Fig. 3 as examples. The decays are non-exponential,

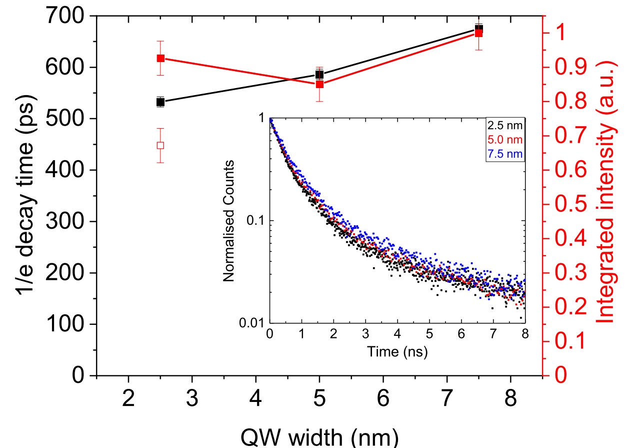


FIG. 3. 10 K spectrally-averaged 1/e decay times (black) and integrated intensities of the QWs with different widths (red closed squares are for MQW, and open square for the SQW). The integrated intensities are normalised to the 7.5 nm sample. Inset are examples of the PL times decays close to the peak energy of the five QW samples, at energies of 2.88 eV, 2.76 eV and 2.70 eV for QW widths of 2.5 nm, 5.0 nm and 7.5 nm.

which is indicative of inhomogeneity in the samples. As discussed above, there is significant indium segregation at SFs and this produces inhomogeneity from the variation in size and in indium content of these regions. The 1/e decay times were extracted and a spectrally weighted mean was calculated for each sample, as shown in Fig. 3. The integrated intensity of the emission at 10 K from each sample is also shown.

The decays are very similar for all samples, and the 1/e decay time varies slowly between 530 ps and 680 ps, and increases with greater QW width. These decay times are similar to those measured for non-polar m-plane wz-InGaN/GaN QWs[26], and also non-polar quantum dots[27], in which recombination is excitonic in nature. This suggests that the zb-InGaN/GaN QWs, and the Qwires within them, are free of the electric fields that tend to separate carriers in wz-InGaN/GaN QWs[28], and that the recombination observed here is hence excitonic in nature[26]. The variation in the decay times is consistent with quantum confinement effects. As the QW width is increased, the exciton binding energy will reduce, and lead to an increase in the decay time[29]. For the MQWs, the variation of integrated intensity is comparable to the uncertainty of the measurement, and is therefore largely unaffected by the QW width, despite the change in recombination lifetime. This suggests that there is no significant competing non-radiative process at low temperature, and the internal quantum efficiency is close to 100 %, as found for wz-InGaN/GaN QWs[30], or that there is a compensating change in the rate of any non-radiative process. In contrast, the integrated intensity for the SQW was about 70 % of the value for the MQW of the same width, sug-

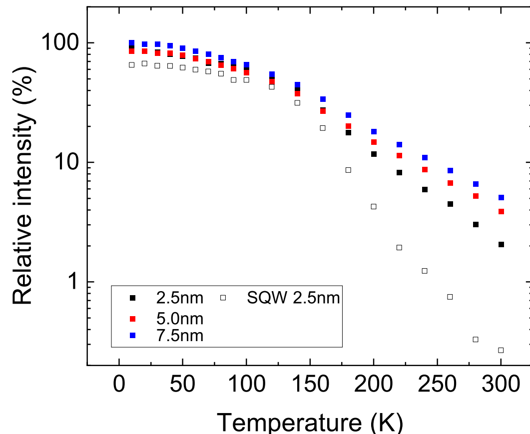


FIG. 4. Integrated intensity for temperatures between 10 K and 300 K, relative to the value for the 7.5 nm MQW sample at 10 K .

gesting the carrier capture is less efficient for the SQW.

The emission efficiency of QWs is typically greatest at low temperature and declines as the temperature is increased [30]. The temperature-dependence of the PL intensity was thus investigated to determine how emission efficiency changes with temperature. For each sample, the integrated intensity at each temperature relative to the value for the 7.5 nm MQW sample at 10 K is shown in Fig. 4.

Between 10 K and 100 K the relative intensity drops slowly from its peak value to about 70 % for all QWs. This quenching process is independent of the QW width and the number of QWs. Above this temperature, the intensity drops more quickly, dropping faster for the narrowest QW, and fastest for the single zb-InGaN/GaN QW sample. The room temperature intensity for the 5.0 nm and 7.5 nm QWs is similar, with values of 4 % and 5 % of the value at 10 K. However, this drops to 2 % for a QW width of 2.5 nm, despite the increase in the radiative recombination rate. The single QW has the lowest relative intensity at room temperature at about 0.2 %.

The emission from the QWs is at a photon energy above the bandgap of both the Si and 3C-SiC in the substrate[31,32] and therefore the effect of re-absorption, and how it varies with temperature, must be considered. At these energies, the 1/e absorption length of Si at room temperature is approximately 1 µm[31]. As the temperature is reduced the absorption length increases but remains of a similar order of magnitude[31]. Since the thickness of the Si is 750 µm, and much larger than the absorption length, all emitted light which enters the Si is reabsorbed and there is no change with temperature. For the 2.7 µm-thick SiC layer the absorption length is 130 µm at room temperature[32], which increases to 170 µm at low temperatures[33]. The amount of re-absorption in this layer is therefore small ($\approx 2$ %), and the change in temperature has been calculated to cause only a 0.5 % change in the extraction efficiency, after accounting for reflections at the hetero-interfaces. These re-absorption effects therefore have no influence on the temperature dependence of the PL measurements, although they will reduce the light extraction efficiency at all temperatures.

The slow initial decrease in intensity from 10 K to 100 K that is independent of the QW width or the number of QWs is attributed to increasing non-radiative recombination at defects as the excitons become more mobile with increasing temperature. A similar slow initial decrease in intensity is observed for polar wz-InGaN/GaN QWs that is also independent of QW width[34], although it can be extended to even higher temperatures by increasing the QW number from 2 to 18 QWs[35]. There are a number of possible explanations for the more rapid intensity decrease at temperatures above 100 K that is stronger for the narrower QWs and for the single QW compared to the 5 QW stacks. One candidate for this process is the thermal escape of electrons from the Coulomb attraction of the hole, separating the exciton. However, as the exciton binding energy will reduce with QW thickness[29], wider QWs would exhibit faster intensity quenching with temperature. In fact, the opposite of this is observed.

Instead, the high temperature quenching is qualitatively consistent with thermionic emission (TE) from the InGaN into the GaN barriers (the dependence on QW number indicating that TE is into the GaN barrier and not just from the Qwires into the rest of the QW). A model of TE out of QWs developed by Schneider and Klitzing [36] shows that increasing the QW width will reduce the TE rate, and will therefore reduce the degree of quenching of the PL intensity. This occurs because increasing the width will reduce the quantum confinement energy, therefore increasing the effective QW barrier height, and also reduce the carrier density in the QW. These results thus suggest that TE of carriers out of the QWs is an important factor in the efficiency of blue-emitting zb-QWs. Hence the efficiency should be improved by adopting strategies to reduce TE in a similar manner to polar-QWs by increasing the number of QWs to increase carrier recapture[35]. Additionally, since increasing the width of the zb-QWs has only a small effect on the radiative recombination rate, this affords a further way to reduce the TE emission rate and thereby increase the room temperature efficiency, as discussed above.

## IV. SUMMARY

In summary, the temperature dependence of PL for zb-InGaN/GaN QWs have been studied, to assess the factors which control the radiative efficiency at room temperature. Increasing the QW width caused the PL spectrum to redshift, and the recombination rate to reduce, consistent with changing the quantum confinement energy of carriers. The constant spectral width for different QW

widths suggest that there is no change in the distribution of radiative states. No significant change in integrated intensity was observed at 10 K for different QW widths, indicating that the recombination is entirely radiative at this temperature, with a lifetime of around 600 ps, which varies slowly with QW width. The magnitude of these lifetimes suggest that the QWs are free of electric fields.

The decrease in intensity with temperature is relative slow and independent of QW width and number until 100 K and then becomes more rapid and dependent on these parameters. This behaviour is attributed to defect-associated non-radiative recombination at prevailing low temperatures with thermionic emission becoming dominant above 100 K. The room temperature efficiency is improved from 0.2 % to 2 % by increasing the number of QWs from one to five, due to greater carrier recapture. Since the radiative lifetime only varies slowly with QW width, the decrease in quantum confinement energy associated with increasing the well width also gives an efficency improvement. Experimentally we see the room temperature efficiency increase to 5 % for 7.5 nm QWs.

Overall, these results indicate that, as well as by increasing the number of QWs in the stack, the efficiency of zb-QWs may also be improved by increasing the well thickness, in contrast to QWs grown in the wz-phase[37]. Moreover, increasing the QW thickness beyond 5 nm only weakly affects the recombination energy, so that using wider wells does not significantly restrict the emission wavelength.

## SUPPLEMENTARY MATERIAL

STEM HAADF image of the single quantum well sample; polarisation-resolved PL spectra and degree of linear polarisation for each QW thickness; calculated recombination energy due to quantum confinement for each QW width and for a range of indium contents.

## ACKNOWLEDGMENTS

This was work funded by EPSRC under grants EP/R010250/1, EP/M010627/1, EP/N01202X/2 and EP/R01146X/1, and Innovate UK under grant 56917-383420.

## DATA AVAILABILITY

Research data supporting this publication are available at DOI: 10.17632/zfbzrb64jt.2.

[1]C. A. Hurni, A. David, M. J. Cich, R. I. Aldaz, B. Ellis, K. Huang, A. Tyagi, R. A DeLille, M. D. Craven, F. M. Steranka, and M. R. Krames, Appl. Phys. Lett. **106**, 031101 (2015).
[2]C. Weisbuch, M. Piccardo, L. Martinelli, J. Iveland, J. Peretti, and J. S. Speck, Phys. Status Solidi A **212**, 899 (2015).
[3]M. Auf der Maur, A. Pecchia, G. Penazzi, W. Rodrigues, and A. Di Carlo, Phys. Rev. Lett. **116**, 027401 (2016).
[4]K. P. O'Donnell, M. Auf der Maur, A. Di Carlo, K. Lorenz, and the SORBET consortium, Phys. Status Solidi RRL **6**, 49 (2012).
[5]S. Hammersley, M. J. Kappers, F. C.-P. Massabuau, S.-L. Sahonta, P. Dawson, R. A. Oliver, and C. J. Humphreys, Appl. Phys. Lett. **107**, 132106 (2015).
[6]H. Okumura , S. Yoshida and T. Okahisa, Appl. Phys. Lett. **64**, 2997 (1994).
[7]D. R. Elsaesser, M. T. Durniak, A. S. Bross, and C. Wetzel, J. Appl. Phys. **122**, 115703 (2017).
[8]S. F. Chichibu, T. Onuma, T. Aoyama, K. Nakajima, P. Ahmet, T. Chikyow, T. Sota, S. P. DenBaars, S. Nakamura, T. Kitamura, Y. Ishida, and H. Okumura, J. Vac. Sci. Technol. B Microelectron. Nanom. Struct. **21**, 1856 (2003).
[9]D. J. As, Microelectronics J. **40**, 204 (2009).
[10]S.-H. Park and Y.-T. Lee, Chinese Phys. Lett. **27**, 044208 (2010).
[11]S. A. Church, B. Ding, P. W. Mitchell, M. J. Kappers, M. Frentrup, G. Kusch, S. M. Fairclough, D. J. Wallis, R. A. Oliver, and D. J. Binks, Appl. Phys. Lett. **117**, 032103 (2020).
[12]S. Li, J. Schörmann, D.J. As, and K. Lischka, Appl. Phys. Lett. **90**, 071903 (2007).
[13]J. Wu, H. Yaguchi, K. Onabe, R. Ito, and Y. Shiraki, Appl. Phys. Lett. **71**, 2067 (1997).
[14]H. Liu, A. C. Frenkel, J. G. Kim, and R. M. Park, J. Appl. Phys. **74**, 6124 (1993).
[15]S. A. Church, S. Hammersley, P. W. Mitchell, M. J. Kappers, S. L. Sahonta, M. Frentrup, D. Nilsson, P. J. Ward, L. J. Shaw, D. J. Wallis, C. J. Humphreys, R. A. Oliver, D. J. Binks, and P. Dawson, Phys. Status Solidi B **1600733**, 1600733 (2017).
[16]H. Okumura, K. Ohta, G. Feuillet, K. Feuillet, S. Chichibu, H. Hamaguchi, P. Hacke, S. Yoshida, J. Cryst. Growth **178**, 113 (1997).
[17]G. Feuillet, F. Widmann, B. Daudin, J. Schuler, M. Arlery, J. L. Rouvière, N. Pelekanos, and O. Briot, Mater. Sci. Eng. B **50**, 233 (1997).
[18]B. Daudin, G. Feuillet, J. Hubner, Y. Samson, F. Widmann, A. Philippe, C. Bru-Chevallier, G. Guillot, E. Bustarret, G. Bentoumi, and A. Deneuville, J. Appl. Phys. **84**, 2295 (1998).
[19]R. M. Kemper, P. Veit, C. Mietze, A. Dempewolf, T. Wecker, F. Bertram, J. Christen, J. K. N. Lindner, and D. J. As, Phys. Status Solidi C **12**, 469 (2015).
[20]L. Y. Lee, M. Frentrup, M. J. Kappers, R. A. Oliver, C. J. Humphreys, and D. J. Wallis, J. Appl. Phys. **124**, 105302 (2018).
[21]R. A. Oliver, F. C. Massabuau, M. J. Kappers, W. A. Phillips, E. J. Thrush, C. C. Tartan, W. E. Blenkhorn, T. J. Badcock, P. Dawson, M. A. Hopkins, D. W. E. Allsopp, and C. J. Humphreys, Appl. Phys. Lett. **103**, 141114 (2013).
[22]J. F. Muth, J. H. Lee, I. K. Shmagin, R. M. Kolbas, H. C. Casey, B. P. Keller, U. K. Mishra, and S. P. DenBaars, Appl. Phys. Lett. **71**, 2572 (1997).
[23]M. Feneberg, M. Röppischer, C. Cobet, N. Esser, J. Schörmann, T. Schupp, D. J. As, F. Hörich, J. Bläsing, A. Krost, and R. Goldhahn, Phys. Rev. B **85**, 155207 (2012).
[24]D. M. Graham, A. Soltani-Vala, P. Dawson, M. J. Godfrey, T. M. Smeeton, J. S. Barnard, M. J. Kappers, C. J. Humphreys, and E. J. Thrush, J. Appl. Phys. **97**, 103508 (2005).
[25]B. Ding, M. Frentrup, S. M. Fairclough, M. J. Kappers, M. Jain, A. Kovács, D. J. Wallis, and R. A. Oliver, J. Appl. Phys. **128**, 145703 (2020).
[26]P. Dawson, S. Schulz, R. A. Oliver, M. J. Kappers, and C. J. Humphreys, J. Appl. Phys. **119**, 181505 (2016).
[27]Z. Gačević, M. Holmes, E. Chernysheva, M. Muller, A. Torres-Pardo, P. Veit, F. Bertram, J. Christen, J. M. G. Calbet, Y. Arakawa, E. Calleja, and S. Lazić, ACS Photonics **4**, 657 (2017).
[28]S. Marcinkevičius, K. M. Kelchner, L. Y. Kuritzky, S. Nakamura, S. P. DenBaars, and J. S. Speck, Appl. Phys. Lett. **103**, 111107 (2013).
[29]J. Feldmann, G. Peter, E. O. Göbel, P. Dawson, K. Moore, C. Foxon, and R. J. Elliott, Phys. Rev. Lett. **59**, 2337 (1987).

[30]S. Watanabe, N. Yamada, M. Nagashima, Y. Ueki, C. Sasaki, Y. Yamada, T. Taguchi, K. Tadatomo, H. Okagawa, and H. Kudo, Appl. Phys. Lett. **83**, 4906 (2003).
[31]G. E. Jellison and F. A. Modine, J. Appl. Phys. **53**, 3745 (1982).
[32]A. Solangi and M. Chaudhry, J. Mater. Res. **7**, 539–541 (1992).
[33]W. Choyke, in *Silicon Carbide–1968*, edited by H. Henisch and R. Roy (Pergamon, 1969) pp. S141 – S152.
[34]J. A. Davidson, P. Dawson, T. Wang, T. Sugahara, J. W. Orton, and S. Sakai, Semicond. Sci. Technol. **15**, 497 (2000).
[35]P. Hurst, P. Dawson, S. Levetas, M. Godfrey, I. Watson, and G. Duggan, Phys. Status Solidi B **228**, 137 (2001).
[36]H. Schneider and K. V. Klitzing, Phys. Rev. B **38**, 6160 (1988).
[37]J. Bai T. Wang and S. Sakai, J. Appl. Phys. **88**, 4729-4733 (2000).